Published online: March 30, 2019

Original Research

High-frequency stimulation of afferent axons alters firing rhythms of downstream neurons

Weijian Ma, Zhouyan Feng*, Zhaoxiang Wang and Wenjie Zhou

Key Laboratory of Biomedical Engineering of Education Ministry, College of Biomedical Engineering & Instrument Science, Zhejiang University, Hangzhou, Zhejiang 310027, China

*Correspondence: fengzy@mail.bme.zju.edu.cn (Zhouyan Feng)

DOI: 10.31083/j.jin.2019.01.18

Deep brain stimulation is an emerging treatment for brain disorders. However, the mechanisms of high-frequency brain stimulation are unclear. Recent studies have suggested that high-frequency stimulation might produce therapeutic effects by eliminating pathological rhythms in neuronal firing. To test the hypothesis, the present study investigated whether stimulation of axonal afferent fibers might alter firing rhythms of downstream neurons in *in-vivo* experiments with Sprague-Dawley rats. Stimulation trains of 100 Hz with one minute duration were applied to the Schaffer collaterals of hippocampus Area CA1 in anaesthetized rats. Spikes of single interneurons and pyramidal neurons in the downstream region were analyzed. The spike rhythms before, during, and after the stimulations were evaluated by analyzing the power spectrum density of autocorrelograms of the spiking sequences. The rhythms of local field potentials were also evaluated by power spectrum density. During baseline recordings, theta rhythms were obvious in the spiking sequences of both types of neuron and in the local field potentials of the stratum radiatum. However, these theta rhythms were all suppressed significantly during the stimulations. Additionally, the results of Pearson's correlation analysis showed that 20-30% variation in the theta rhythms of neuronal firing could be explained by changes of the theta rhythms in local field potentials. High-frequency axonal stimulation might prevent the original rhythmic excitation in afferent fibers and generate new excitation by stimulation pulses *per se*, thereby suppressing the theta rhythms of individual neuron firing and of local field potentials in the region downstream from stimulation. The results provide new evidence to support the hypothesis that high-frequency stimulation can alter the firing rhythms of neurons, which may underlie the therapeutic effects of deep brain stimulation.

Keywords

Deep brain stimulation; high frequency stimulation; unit spike; theta rhythm; local field potential; autocorrelogram; power spectrum density; axonal block; hippocampus area CA1

Abbreviations

DBS	Deep brain stimulation
HFS	High-frequency stimulation
PSD	Power spectrum density
LFP	Local field potentials
RE	Recording electrode
SE	Stimulating electrode
PS	Population spike
fEPSP	Field excitatory postsynaptic potential
Pyr. layer	Pyramidal cell layer
S. rad.	Stratum radiatum
MUA	Multiple unit activity

1. Introduction

Deep brain stimulation (DBS) has been successfully utilized for treating neurological diseases such as Parkinson's disease and epilepsy (Vonck et al., 2013; Cury et al., 2017). DBS has also shown potential in the treatment of mental disorders such as refractory obsessive-compulsive disorder and depression (Pereira et al., 2012; Taghva et al., 2013). Investigations have shown that therapeutic DBS requires the use of electrical pulse trains with a high frequency in the range of 90-185 Hz (Kuncel et al., 2006; Birdno et al., 2012). However, the mechanisms of high frequency stimulation (HFS) have not yet been determined. This has limited the clinical application of DBS for treatment of new diseases (Udupa and Chen, 2015; Chiken and Nambu, 2016).

Three potential mechanisms of HFS on neuronal activity have been proposed: inhibition, excitation, and modulation. Studies have shown that HFS may suppress neuronal firing by activation of the inhibitory synapses of neural circuits (Alhourani et al., 2015), or by depletion of the neurotransmitters of excitatory synapses (Iremonger et al., 2006). However, other studies that involved animal experiments and mathematical simulations have shown that HFS may increase the firing rate of neuronal action potentials (Deniau et al., 2010). The paradoxical increase and decrease of neuronal activity induced by HFS may be unraveled by a third plausible mechanism, that of modulation. HFS may exert efficacy by changing firing patterns or firing rhythms of neurons rather than purely changing neuronal firing rates (McConnell et al., 2012; Florence et al., 2016; Herrington et al., 2016).

Journal of Integrative Neuroscience

Neurons in the brain often fire action potential sequences in rhythmic patterns. Additionally, pathological rhythms are features of many brain disorders (Buzsáki, 2002; Buzsáki and Draguhn, 2004). For instance, the theta rhythmic firing of hippocampal neurons may be related to the development of epilepsy (Kitchigina et al., 2013). Abnormal theta and beta rhythms of neuronal firing have been considered as features of Parkinson's disease. The theta rhythm may play an important role in the generation of abnormal tremors (Tass et al., 2010; Singh et al., 2016). Recent studies have suggested that HFS may change the patterns of action potential firing by various neurons. During HFS, new patterns of neuronal activity might replace and mask the pathological rhythms of neurons, thereby achieving therapeutic effect (So et al., 2012; Rosenbaum et al., 2014). Thus, a potential mechanism for DBS might be the suppression effect of HFS on rhythms of neuronal firing.

To test the hypothesis, trains of HFS pulses were applied to the Schaffer collaterals, the afferent fiber tracts of the hippocampus Area CA1, in anaesthetized rats. Single unit activity of both interneurons and pyramidal neurons in the region downstream fron stimulation was analyzed to determine whether the axonal HFS could change the rhythmic firing of downstream neurons.

Axons can widely modulate neuronal activity in downstream regions through their fiber projections. Additionally, compared to other components of neurons, axons are more prone to be activated by narrow HFS pulses (Ranck, 1975). Therefore, the investigation of neuronal responses to axonal HFS could reveal important information for DBS application. Additionally, the hippocampal region was chosen for investigation of the mechanisms of HFS because it is one of the DBS targets for the treatment of neurological diseases such as refractory epilepsy and Alzheimer's disease (Jiruska et al., 2010; Sankar et al., 2015). The results of this study might provide new evidence for a theory of HFS modulation.

2. Materials and methods

2.1 Animal surgery and electrode placement

Experiments were approved by the Institutional Animal Care and Use Committee, Zhejiang University. Seven adult male Sprague-Dawley rats (260-340 g) were each anesthetized with urethane (1.25 g/kg, i.p.) and placed in a stereotaxic apparatus (Stoelting Co., USA). The anesthetic state was monitored by pinching rat feet and observing rat responses. Body temperature was maintained at $\sim$ 37°C. The nasal skin was cut and two stainless-steel screws were fixed in the nasal bone to serve as the reference and ground electrodes.

The scalp was opened and partial skull was removed to allow the placement of a recording electrode (RE) and a stimulating electrode (SE). The RE was a 16-channel (2*8) electrode array (Model Poly2, Neuro-Nexus Technologies, USA) positioned in hippocampus Area CA1 (AP: 3.5 mm, ML: 2.7 mm, DV: $\sim$ 2.5 mm). The SE was a concentric bipolar stainless-steel electrode (Model CBCSG75, FHC, USA) positioned in the Schaffer collaterals of the hippocampus Area CA1 (AP: 2.2 mm, ML: 2.0 mm, DV: $\sim$ 2.8 mm). According to the clear lamellar organizations of neuronal structures in hippocampus, the final positions of electrodes were determined based on the waveforms of orthodromically-evoked potentials as well as unit spike signals that appeared serially in the 16 channel recording array (Kloosterman et al., 2001; Feng et al., 2013). Specifically, a single stimulation pulse on the Schaffer collaterals could induce a population spike (PS) and a field excitatory postsynaptic potential (fEPSP) in the downstream pyramidal cell layer (Pyr. layer) and stratum radiatum (S. rad.), respectively. The distance between the two layers was $\sim$ 0.4 mm (Fig. 1A).

At the end of experiments, the rats were euthanised by intraperitoneal over-dose injection of urethane followed by injection of a saturated KCl solution directly into the heart.

2.2 Recording and stimulating

Raw signals from the recording electrode with a frequency range of 0.3-5000 Hz were amplified $\times$ 100 with a 16-channel extracellular amplifier (Model 3600, A-M System Inc., USA). The amplified signals were then sampled by a ML880 PowerLab data acquisition system (ADInstruments Inc., Australia) with a sampling rate of 20 kHz and an A/D conversion resolution of 16 bits.

Stimulations were 100 Hz biphasic current pulses with a pulse width of 0.1 ms and duration of 1 min, generated by an isolated pulse stimulator (Model 3800, A-M System Inc., USA). Current intensity was set at 0.3-0.5 mA to evoke an approximately 75% maximal amplitude PS according to the input-output curve of single pulse stimulation.

2.3 Analysis of single unit spikes

Four neighboring channels of the recording array located in the pyramidal layer were used to extract the unit spikes of neuronal firing as described previously (Feng et al., 2017). Briefly, HFS stimulation artifacts were removed by a linear interpolation algorithm (Yu et al., 2016): a signal segment of 1.5 ms around each artifact of a stimulation pulse was replaced by a short linear interpolation that connected the two endpoints of the artifact segment. Next, the artifact-free signals were filtered ($>$ 500 Hz) by a high-pass digital filter (LabChart v7.0 software, ADInstruments Inc., Australia) to remove the local field potential (LFP) in the low-frequency band and to obtain multiple unit activity (MUA). Unit spikes in the MUA signals were then detected by an amplitude threshold of about $\times$ 3-5 the signal standard deviation (Vargas-Irwin et al., 2007). Finally, feature vectors of the spike waveforms (first principal components and amplitudes) were used to sort the spikes of multiple neurons with open-source clustering software (SpikeSort 3D, Neuralynx Inc, www.Neuralynx.com). Histograms of inter-spike intervals of the sorted unit spikes were used to verify the clustering results of single unit spikes (Barthó et al., 2004).

According to the waveform features of spikes of interneurons and pyramidal neurons, single unit spikes of different neurons were distinguished (Feng et al., 2017). Briefly, half widths (measured from the negative peak to the post-positive peak) of the mean spike waveforms of different neurons were evaluated. Neurons with spike half widths of $<$ 0.4 ms and $>$ 0.7 ms were defined as putative interneurons and pyramidal neurons, respectively (Barthó et al., 2004).

2.4 Rhythm analysis

To investigate the effect of axonal HFS on the theta rhythms of neuronal firing, autocorrelation histograms of the binary sequences of unit spikes were generated to calculate power spectrum density (PSD) in the periods before, during, and after HFS

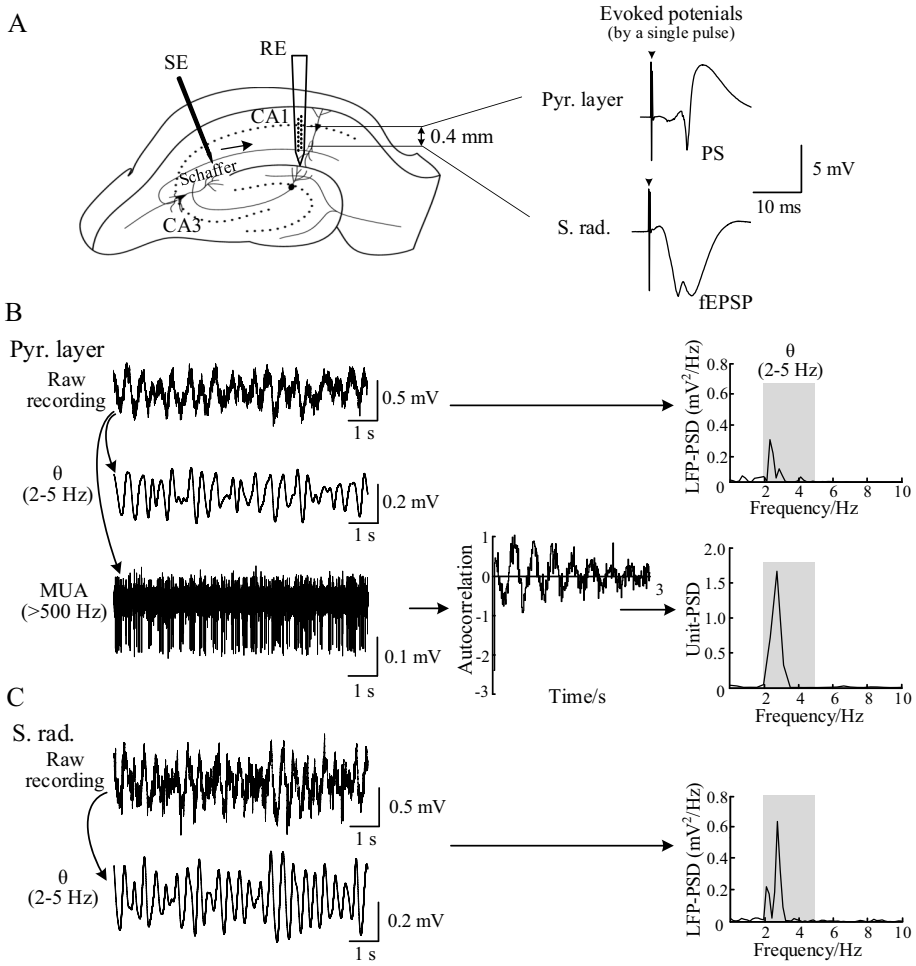

Figure 1. Spontaneous theta rhythms of neuronal firing in hippocampus Area CA1 of anaesthetized rats. (A) *Left*: Schematic diagram of the rat hippocampus and electrode location. Recording electrode (RE) and stimulating electrode (SE) were respectively located in hippocampus Area CA1 and in the upstream Schaffer collaterals. Arrow indicates direction of stimulus-induced excitation. Electrical signals in the pyramidal layer (Pyr. layer) and in the stratum radiatum (S. rad.) were collected by two recording sites in the RE array (separated by 0.4 mm). *Right*: Typical waveforms of the population spike (PS) and field excitatory postsynaptic potential (fEPSP) evoked by a stimulus and recorded in Pyr. and S. rad. layers, respectively. Inverted triangles: Truncated stimulus artifacts. (B) *Left*: Segment of raw recording in the Pyr. layer together with associated local field potential (LFP) in theta range and multiple unit activity (MUA). *Middle*: Autocorrelation profile of the sequence of unit spikes extracted from the MUA. *Right*: Corresponding LFP-power spectrum density (top: LFP-PSD) and unit spike-power spectrum density (bottom: unit-PSD). (C) *Left*: Recording from S. rad. corresponding to the segment in (B) with its LFP in theta range. *Right*: Corresponding LFP-power spectrum density. Shaded area: Theta range (2–5 Hz).

(Kitchigina et al., 2003, 2013). The length of autocorrelograms was three seconds with a temporal resolution of two milliseconds. The mean component in autocorrelograms was removed and the values were then normalized to eliminate the influence of spike rates. To analyze rhythms in the sequences of unit spikes by autocorrelogram, the PSD of autocorrelograms (unit-PSDs) was calculated by Welch's modified periodogram method with a Hanning window, an overlap of 50%, and a frequency resolution of 0.49 Hz.

Additionally, PSD curves of LFP in both the pyramidal layer and the stratum radiatum were calculated in the frequency range of 0-10 Hz to evaluate the theta rhythms in the LFP. The frequency resolution of LFP-PSD was 0.15 Hz.

Cumulative PSD power in the frequency range of theta rhythm (2-5 Hz) was calculated for both unit-PSD and LFP-PSD to evaluate the intensity of theta rhythm.

All statistical data were represented as mean ± standard deviation. Statistical significance of the difference between HFS data and the corresponding baseline data were tested by paired *t*-test. Pearson's correlation analysis was used to test the linear correlation between the theta rhythms of unit-PSD and the theta rhythms of LFP-PSD. The significance level was set at $p < 0.05$.

3. Results

3.1 Spontaneous theta rhythms of neurons in the hippocampus Area CA1 of anesthetized rats

Previous studies have shown that theta rhythms of the LFP commonly appeared in the hippocampus of urethane anesthetized

rats with frequencies of 2-5 Hz (Buzsáki, 2002). In the present study, the baseline recording in the pyramidal layer of Area CA1 clearly showed a rhythm with a peak of 2.3 Hz in the LFP-PSD (Fig. 1B *Top*). Meanwhile, the unit spikes of MUA fired in clusters and were obviously rhythmic in the autocorrelogram of the spike sequence. A peak at 2.7 Hz appeared in the unit-PSD of the autocorrelogram, indicating a theta rhythm in the spontaneous firing of neuronal action potentials (Fig. 1B *Bottom*). Additionally, the baseline recording in the stratum radiatum showed a clear rhythm with a peak of 2.75 Hz in LFP-PSD (Fig. 1C). The peak power density value 0.63 mV^2/Hz in the LFP-PSD of stratum radiatum was greater than the peak value 0.29 mV^2/Hz in the LFP-PSD of pyramidal layer, indicating a stronger theta rhythm in the LFP of stratum radiatum (Fig. 1B and Fig. 1C).

3.2 HFS changed the rhythms in neuronal firing

To investigate the effects of HFS on the rhythms of neuronal firing, one minute of 100 Hz HFS trains were applied to the Schaffer collaterals of the hippocampus Area CA1 (Fig. 2). During HFS, in the pyramidal layer, the MUA increased and the theta rhythms of LFP decreased (Fig. 2A). The theta rhythms of LFP in the stratum radiatum also decreased significantly during HFS (Fig. 2B).

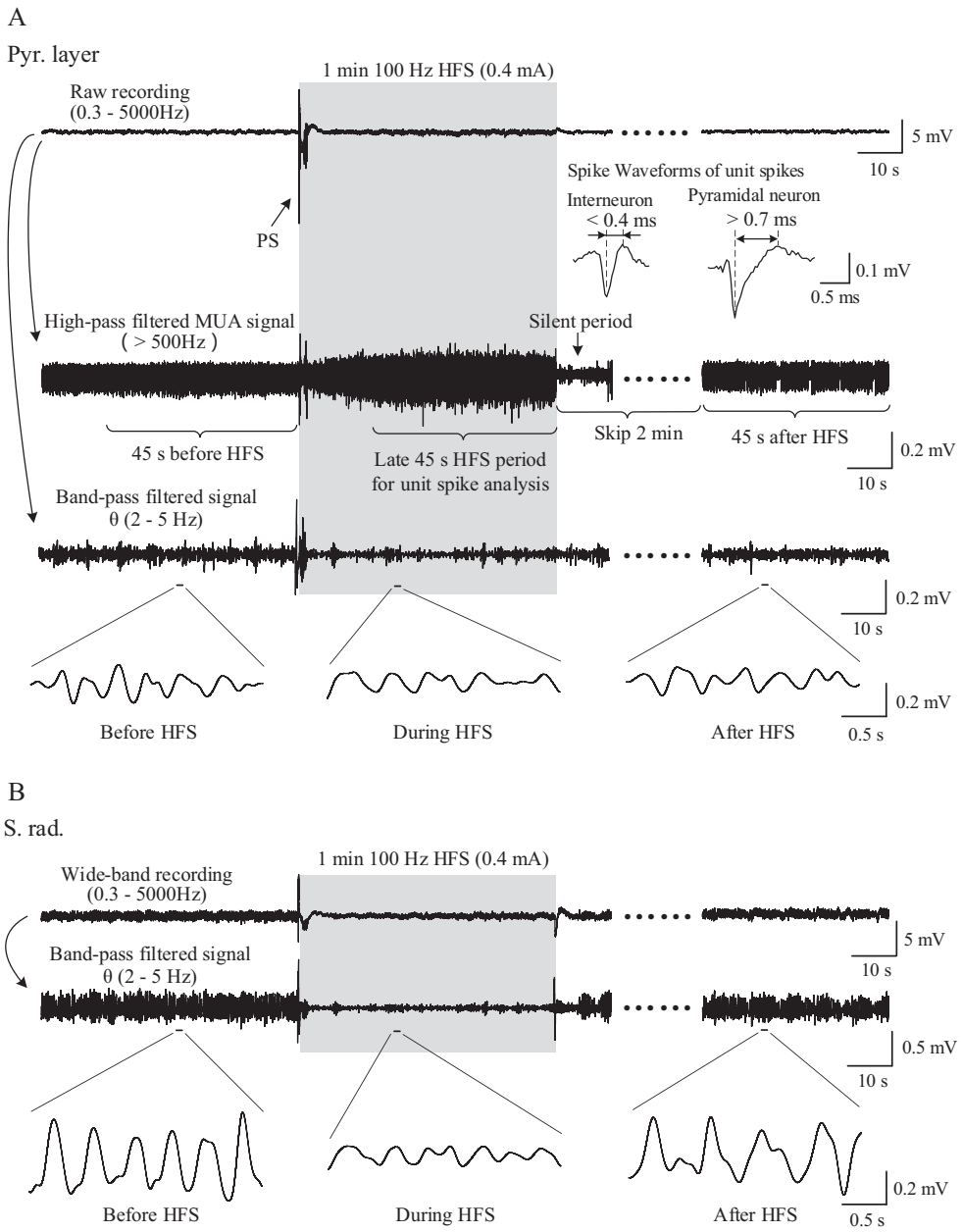

Figure 2. Changes in the multiple unit activity and local field potential evoked by stimulation (one minute, 100 Hz). (A) Example recording from Pyr. layer and associated multiple unit activity and local field potential in theta range. Typical spike waveforms of interneurons and pyramidal neurons are given in the two expanded insets. (B) Corresponding recording from S. rad. layer. Shaded area: High-frequency stimulation period, stimulus artifacts removed.

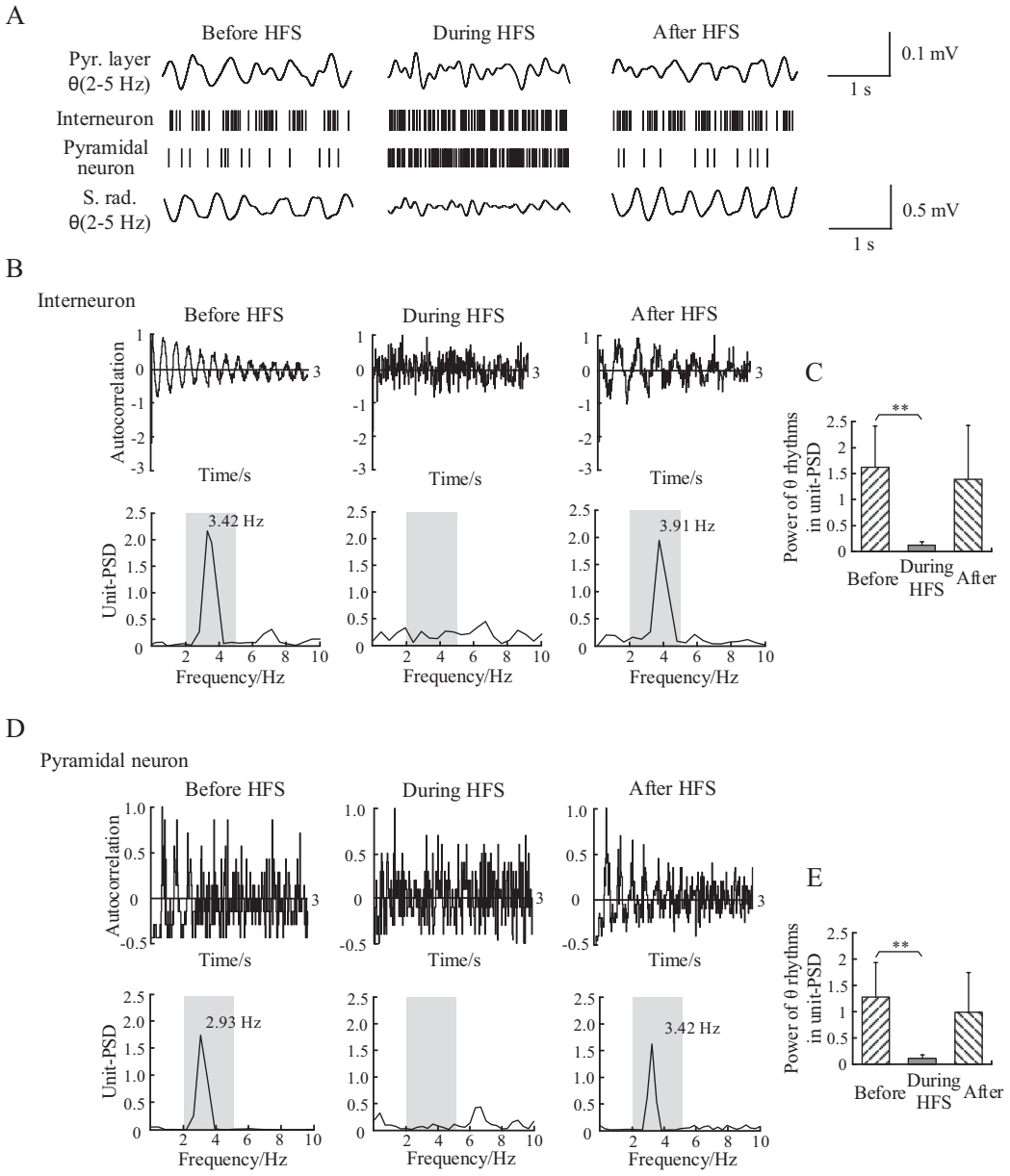

Figure 3. Axonal stimulation suppressed theta rhythms in neuronal firing. (A) *Top to bottom*: Examples of theta signal recorded from Pyr. layer, raster plots of unit spikes of an interneuron and a pyramidal neuron, and theta signal from S. rad. during the three periods of: before, during, and after high-frequency stimulation, respectively. (B) Example autocorrelation profiles and their unit-power spectrum densities (unit-PSD) for interneuron spikes during the three different periods. (C) Statistical power of theta rhythms in unit-PSD of interneurons during the three different periods. Paired *t*-test was used to compare mean power during stimulation and baseline mean power prior to stimulation (** $p < 0.01$, $n = 7$). (D) and (E) Corresponding data for pyramidal neurons.

The late 45 s period of MUA signals during one minute HFS was used to analyze unit spikes to avoid interference from the large PS events at the onset of HFS (Feng et al., 2013). Accordingly, the 45 s period of baseline signal immediately before HFS was used as a baseline control. A 45 s period of MUA signals starting from two minutes after the termination of HFS was selected to analyze firing recovery (Fig. 2A). The two minute period immediately following HFS was skipped because the firing of unit spikes would stop for tens of seconds and then gradually recove during this period (Feng et al., 2017).

Unit spikes of interneurons and pyramidal neurons in seven rat experiments were analyzed. An example of the raster plots of unit spikes (Fig. 3A) shows that before HFS, the firing of an interneuron was clustered synchronously with the theta rhythm of LFP in the pyramidal layer and stratum radiatum, indicating a rhythmic firing. However, during HFS, this firing rhythm disappeared despite an increase in the firing rate of the interneuron. After HFS, the rhythm recovered. The suppression of rhythmic firing by HFS was more obvious in the autocorrelograms and in the unit-PSD plots of the interneuron (Fig. 3B). A peak appeared at 3.4 Hz in

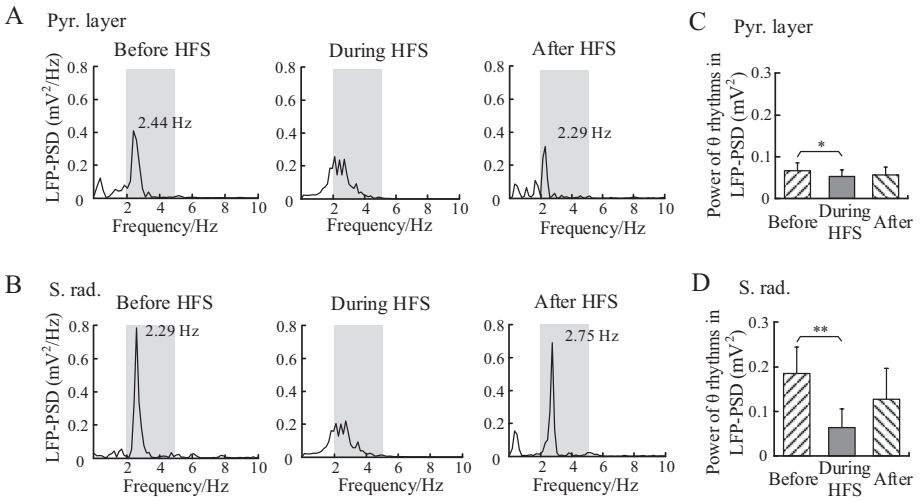

Figure 4. Axonal stimulation suppressed theta rhythms in the local field potential. (A) and (B) Examples of local field potential-power spectrum densities in Pyr. layer (A) and S. rad. (B) for the three different periods: before, during, and after stimulation. (C) and (D) Statistical comparison of the power of theta rhythms (2–5 Hz) for the three different periods. $^{*}p < 0.05$, $^{**}p < 0.01$, paired t-test, $n = 7$.

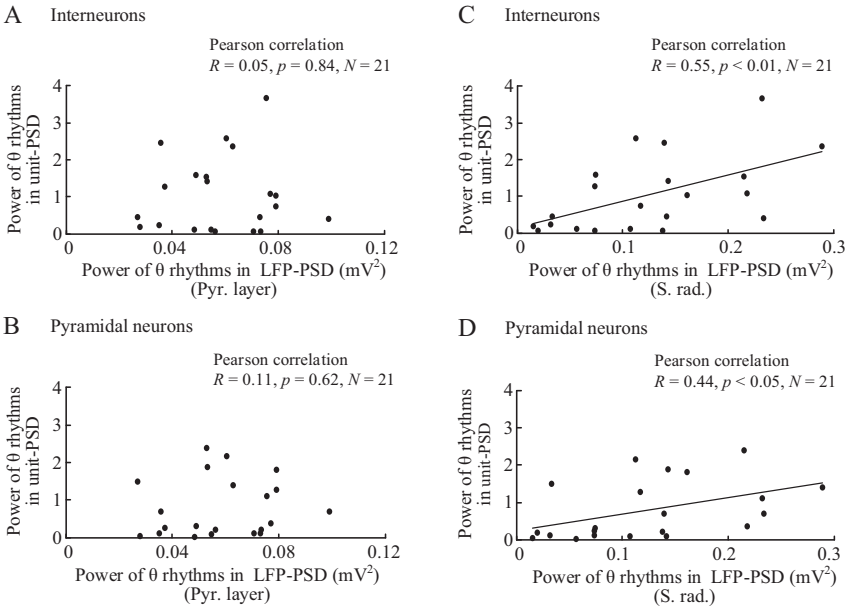

Figure 5. Correlation between theta rhythm of neuronal firing and theta rhythm of local field potential. Scatter diagrams of theta power of unit spikes (A and C for interneurons, B and D for pyramidal neurons) against the corresponding theta power of local field potential (A and B for Pyr. Layer, C and D for S. rad.). Pearson's correlation coefficient (R) is shown above each plot together with the p-value. The data number ($N = 3 \times 7 = 21$) is the number of pooled data from the three different periods of before, during, and after stimulation within the seven experiments.

the unit-PSD before HFS disappeared during HFS and reappeared at 3.9 Hz after HFS. The mean power of theta rhythms in unit-PSD of interneurons was significantly decreased from 1.62 ± 0.79 before HFS to 0.12 ± 0.06 during HFS ($p < 0.01$, paired t-test, $n = 7$) and recovered to 1.39 ± 1.04 after HFS (Fig. 3C).

Rhythmic firing of pyramidal neurons was not obvious in raster plots because of their low spontaneous firing rates (Fig. 3A). However, the theta rhythms in their firing before and after HFS were obvious in the corresponding autocorrelograms and unit-PSD plots (Fig. 3D). The suppression of rhythmic firing during HFS was statistically significant as the mean power of theta rhythms in the unit-PSD of pyramidal neurons decreased from 1.29 ± 0.65 before HFS to 0.11 ± 0.07 during HFS ($p < 0.01$, paired t-test, $n = 7$) and recovered to 0.99 ± 0.76 after HFS (Fig. 3E).

HFS also suppressed theta rhythms in LFP signals (Fig. 4). For LFP of baseline recordings before HFS, peaks of theta rhythms were obvious in LFP-PSD of both the pyramidal layer and the stratum radiatum. The peaks decreased during HFS and recovered after HFS (Fig. 4A and 4B). The mean power of theta rhythms in LFP-PSD of the pyramidal layer significantly decreased from 0.067 ± 0.019 mV^2 before HFS to 0.052 ± 0.016 mV^2 during HFS ($p < 0.05$, paired t-test, $n = 7$; Fig. 4C). Similarly, the mean power

of theta rhythms in LFP-PSD of the stratum radiatum significantly decreased from 0.185 ± 0.058 mV^2 before HFS to 0.063 ± 0.043 mV^2 during HFS ($p < 0.01$, paired t-test, $n = 7$; Fig. 4D). Additionally, in baseline recordings, the mean power of theta rhythms in LFP-PSD of the stratum radiatum (0.185 ± 0.058 mV^2) was significantly larger than that of the pyramidal layer (0.067 ± 0.019 mV^2; $p < 0.01$, paired t-test, $n = 7$). However, there was no significant difference in the LFP theta rhythms of the two layers during HFS.

These results indicate that axonal HFS could suppress the theta rhythm activity of both downstream interneurons and pyramidal neurons. Simultaneously, HFS decreased theta rhythms in the LFP of different layers of the hippocampus Area CA1. This suggests that changes in the theta rhythms of unit spikes might be related to changes of LFP rhythms. Therefore, the relationship between the power of theta rhythms of neuronal firing and the power of theta rhythms of LFP was next evaluated.

3.3 Rhythms in the LFP of stratum radiatum could modulate the neuronal firing

To investigate the relationship between the theta rhythms of neuronal firing and those of LFP, the data of theta power in the three periods (before, during, and after HFS) were pooled together and Pearson's correlation coefficient was calculated (Fig. 5). For the LFP in the pyramidal layer, there were no significant correlations between the power of theta rhythms of neuronal firing (neither the interneurons nor the pyramidal neurons) and the power of LFP theta rhythms (Fig. 5A and 5B). However, for LFP in stratum radiatum, significant correlations were observed between the power of theta rhythms of both types of neuron and the power of LFP theta rhythms (Fig. 5C and 5D).

These results indicate that changes of neuronal firing rhythms were related to the LFP of the stratum radiatum (located hundreds of microns away from the neuronal somata) rather than the LFP of the pyramidal layer that immediately surrounded the neuronal somata. This was attributed to the fact that stratum radiatum contains excitatory synaptic terminals of afferent axons.

4. Discussion

This study indicates that axonal HFS of afferent Schaffer collaterals can suppress the low-frequency (theta) rhythms of neuronal firing for both interneurons and pyramidal neurons downstream in hippocampus Area CA1. The decrease of rhythmic firing is related to a decrease in LFP rhythms of the stratum radiatum where the excitatory afferent fiber synaptic terminals are located. Possible mechanisms of these results are now discussed.

During pre-HFS baseline recordings, spontaneous theta rhythms appeared both in the unit spike sequences of neuronal firing and in the LFP of different layers (pyramidal layer, stratum radiatum) in hippocampus Area CA1 (Fig. 1, Fig. 3 and Fig. 4). These observations were consistent with previous studies that have indicated correlation between the rhythms of neuronal firing and LFP (Buzsáki and Draguhn, 2004). The LFP theta rhythms may be an epiphenomenon of the rhythmic firing of CA1 neurons (Buzsáki, 2002; Rutishauser et al., 2010). Studies have shown that the theta rhythms of CA1 neurons may have several origins, including rhythmic inputs from the neuronal populations upstream in Area CA3, excitatory inputs from the entorhinal cortex, and oscillations of calcium currents via voltage-dependent ionic channels of synapses in the stratum radiatum of pyramidal neurons (Lee et al., 1994; Kamondi et al., 1998; Buzsáki, 2002; Kitchigina et al., 2003; Huh et al., 2010; Buzsáki and Moser, 2013). The rhythmic inputs from upstream CA3 neurons may result in the LFP power of theta rhythms in the stratum radiatum being significantly greater than in the pyramidal layer (Fig. 1 and Fig. 4).

Axonal HFS may decrease rhythmic excitation originating from the upstream projections to downstream neurons. Schaffer collaterals, the stimulation target of the present study, are the major pathway between Areas CA3 and CA1. Axonal HFS at the Schaffer collaterals may prevent the propagation of theta rhythmic activity from Area CA3 to CA1 through the mechanism of HFS-induced depolarization block at axons (Bellinger et al., 2008; Jensen and Durand, 2009; Feng et al., 2013), thereby decreasing the LFP theta rhythms in Area CA1 (Fig. 4). Presumably, this attenuation of rhythmic driving may result in a decrease of theta rhythms in neuronal firing. This speculation is supported by the significant correlation between changes of theta rhythmic firing and the changes of LFP theta rhythms in the stratum radiatum where Schaffer collateral inputs were located (Fig. 5). However, the determination coefficients (R^2) of correlation analysis were only 20-30%, which indicates that decreased rhythmic driving by upstream neurons could only explain a fraction of the alteration of rhythmic theta firing.

HFS pulses *per se* could have excitatory effects on downstream neurons, which might be another origin of decreases in the theta rhythms of neuronal firing. Prolonged HFS can cause axons to fail to generate action potentials following every stimulus pulse because of depolarization block. However, the axonal block is only partial and axons can still intermittently fire action potentials (Guo et al., 2018). These HFS-induced activations can propagate along axons to finally activate downstream post-synaptic neurons. They may then modulate neuronal firing in a de-synchronized manner (Feng et al., 2017; Wang et al., 2018), thereby eliminating theta rhythms.

A limitation of the present study is that the data were obtained from urethane anesthetized rats. The anesthetic could slightly decrease the firing rate of pyramidal cells (Mercer et al., 1978) and also slightly lower the frequency of theta rhythms in the hippocampus (Buzsáki, 2002). However, the suppression of theta rhythm firing of neurons by axonal HFS may well be similar under both anesthetized and awake conditions provided rhythmic firing exists.

5. Conclusion

The present study shows that HFS of afferent axons in the rat hippocampus suppresses rhythmic firing of downstream neurons. Two major mechanisms may underlie the suppression effects. First, HFS-induced axonal failures may prevent the propagation of theta rhythmic activity from its origins to downstream neurons. Second, HFS pulses *per se* may change the firing patterns of downstream neurons through the excitatory effects that leak from partially blocked axons. These mechanisms of axonal HFS provide new insights into how DBS could change neuronal firing patterns.

Authorship contribution

Weijian Ma and Zhouyan Feng designed the study. Weijian Ma, Wenjie Zhou and Zhaoxiang Wang performed the experiments and analyzed the data. Weijian Ma and Zhouyan Feng wrote and revised the manuscript.

Acknowledgements

This work was supported by the National Natural Science Foundation of China (No. 30970753) and by Major Scientific Project of Zhejiang Lab (No. 2018DG0ZX01).

Conflict of interest

The authors declare no competing interests.

Submitted: January 23, 2018
Accepted: March 28, 2019
Published: March 30, 2019

References

Alhourani, A., McDowell, M. M., Randazzo, M. J., Wozny, T. A., Kondylis, E. D., Lipski, W. J., Beck, S., Karp, J. F., Ghuman, A. S. and Richardson, R. M. (2015) Network effects of deep brain stimulation. *Journal of Neurophysiology* **114**, 2105-2117.

Barthó, P., Hirase, H., Monconduit, L., Zugaro, M., Harris, K. D. and Buzsáki, G. (2004) Characterization of neocortical principal cells and interneurons by network interactions and extracellular features. *Journal of Neurophysiology* **92**, 600-608.

Bellinger, S. C., Miyazawa, G. and Steinmetz, P. N. (2008) Submyelin potassium accumulation may functionally block subsets of local axons during deep brain stimulation: a modeling study. *Journal of Neural Engineering* **5**, 263-274.

Birdno, M. J., Kuncel, A. M., Dorval, A. D., Turner, D. A., Gross, R. E. and Grill, W. M. (2012) Stimulus features underlying reduced tremor suppression with temporally patterned deep brain stimulation. *Journal of Neurophysiology* **107**, 364-383.

Buzsáki, G. (2002) Theta oscillations in the hippocampus. *Neuron* **33**, 325-340.

Buzsáki, G. and Draguhn, A. (2004) Neuronal oscillations in cortical networks. *Science* **304**, 1926-1929.

Buzsáki, G. and Moser, E. I. (2013) Memory, navigation and theta rhythm in the hippocampal-entorhinal system. *Nature Neuroscience* **16**, 130-138.

Chiken, S. and Nambu, A. (2016) Mechanism of deep brain stimulation: inhibition, excitation, or disruption? *Neuroscientist* **22**, 313-322.

Cury, R.G., Fraix, V., Castrioto, A., Perez, F. M., Krack, P., Chabardes, S., Seigneuret, E., Alho, E., Benabid, A. L. and Moro, E. (2017) Thalamic deep brain stimulation for tremor in Parkinson disease, essential tremor, and dystonia. *Neurology* **89**, 1416-1423.

Deniau, J. M., Degos, B., Bosch, C. and Maurice, N. (2010) Deep brain stimulation mechanisms: beyond the concept of local functional inhibition. *European Journal of Neuroscience* **32**, 1080-1091.

Feng, Z., Zheng, X., Yu, Y. and Durand, D. M. (2013) Functional disconnection of axonal fibers generated by high frequency stimulation in the hippocampal CA1 region *in-vivo*. *Brain Research* **1509**, 32-42.

Feng, Z., Wang, Z., Guo, Z., Zhou, W., Cai, Z. and Durand, D. M. (2017) High frequency stimulation of afferent fibers generates asynchronous firing in the downstream neurons in hippocampus through partial block of axonal conduction. *Brain Research* **1661**, 67-78.

Florence, G., Sameshima, K., Fonoff, E. T. and Hamani, C. (2016) Deep brain stimulation: more complex than the inhibition of cells and excitation of fibers. *Neuroscientist* **22**, 332-345.

Guo, Z., Feng, Z., Wang, Y. and Wei, X. (2018) Simulation study of intermittent axonal block and desynchronization effect induced by high-frequency stimulation of electrical pulses. *Frontiers in Neuroscience* **22**, 1-12.

Herrington, T. M., Cheng, J. J. and Eskandar, E. N. (2016) Mechanisms of deep brain stimulation. *Journal of Neurophysiology* **115**, 19-38.

Huh, C. Y., Goutagny, R. and Williams, S. (2010) Glutamatergic neurons of the mouse medial septum and diagonal band of Broca synaptically drive hippocampal pyramidal cells: relevance for hippocampal theta rhythm. *Journal of Neuroscience* **30**, 15951-15961.

Iremonger, K. J., Anderson, T. R., Hu, B. and Kiss, Z. H. (2006) Cellular mechanisms preventing sustained activation of cortex during subcortical high-frequency stimulation. *Journal of Neurophysiology* **96**, 613-621.

Jensen, A. L. and Durand, D. M. (2009) High frequency stimulation can block axonal conduction. *Experimental Neurology* **220**, 57-70.

Jiruska, P., Powell, A. D., Deans, J. K. and Jefferys, J. G. (2010) Effects of direct brain stimulation depend on seizure dynamics. *Epilepsia* **51**, 93-97.

Kamondi, A., Acsady, L., Wang, X. J. and Buzsáki, G. (1998) Theta oscillations in somata and dendrites of hippocampal pyramidal cells *in vivo*: activity-dependent phase-precession of action potentials. *Hippocampus* **8**, 244-261.

Kitchigina, V., Kutyreva, E. and Brazhnik, E. (2003) Modulation of theta rhythmicity in the medial septal neurons and the hippocampal electroencephalogram in the awake rabbit via actions at noradrenergic alpha 2-receptors. *Neuroscience* **120**, 509-521.

Kitchigina, V., Popova, I., Sinelnikova, V., Malkov, A., Astasheva, E., Shubina, L. and Aliev, R. (2013) Disturbances of septohippocampal theta oscillations in the epileptic brain: reasons and consequences. *Experimental Neurology* **247**, 314-327.

Kloosterman, F., Peloquin, P. and Leung, L. S. (2001) Apical and basal orthodromic population spikes in hippocampal CA1 *in vivo* show different origins and patterns of propagation. *Journal of Neurophysiology* **86**, 2435-2444.

Kuncel, A. M., Cooper, S. E., Wolgamuth, B. R., Clyde, M. A., Snyder, S. A., Montgomery, E. J., Rezai, A. R. and Grill, W. M. (2006) Clinical response to varying the stimulus parameters in deep brain stimulation for essential tremor. *Movement Disorders* **21**, 1920-1928.

Lee, M. G., Chrobak, J. J., Sik, A., Wiley, R. G. and Buzsáki, G. (1994) Hippocampal theta activity following selective lesion of the septal cholinergic system. *Neuroscience* **62**, 1033-1047.

McConnell, G. C., So, R. Q., Hilliard, J. D., Lopomo, P. and Grill, W. M. (2012) Effective deep brain stimulation suppresses low-frequency network oscillations in the basal ganglia by regularizing neural firing patterns. *Journal of Neuroscience* **32**, 15657-15668.

Mercer, L. J., Remley, N. R. and Gilman, D. P. (1978) Effects of urethane on hippocampal unit activity in the rat. *Brain Research Bulletin* **3**, 567-570.

Pereira, E. A., Green, A. L., Stacey, R. J. and Aziz, T. Z. (2012) Refractory epilepsy and deep brain stimulation. *Journal of Clinical Neuroscience* **19**, 27-33.

Ranck, J. J. (1975) Which elements are excited in electrical stimulation of mammalian central nervous system: a review. *Brain Research* **98**, 417-440.

Rosenbaum, R., Zimnik, A., Zheng, F., Turner, R. S., Alzheimer, C., Doiron, B. and Rubin, J. E. (2014) Axonal and synaptic failure suppress the transfer of firing rate oscillations, synchrony and information during high frequency deep brain stimulation. *Neurobiology of Disease* **62**, 86-99.

Rutishauser, U., Ross, I. B., Mamelak, A. N. and Schuman, E. M. (2010) Human memory strength is predicted by theta-frequency phase-locking of single neurons. *Nature* **464**, 903-907.

Sankar, T., Chakravarty, M. M., Bescos, A., Lara, M., Obuchi, T., Laxton, A. W., McAndrews, M. P., Tang-Wai, D. F., Workman, C. I., Smith, G. S. and Lozano, A. M. (2015) Deep brain stimulation influences brain structure in Alzheimer's disease. *Brain Stimulation* **8**, 645-654.

Singh, A., Mewes, K., Gross, R. E., DeLong, M. R., Obeso, J. A. and Papa, S. M. (2016) Human striatal recordings reveal abnormal discharge of projection neurons in parkinson's disease. *Proceedings of the National Academy of Sciences of the United States of America* **113**, 9629-9634.

So, R. Q., Kent, A. R. and Grill, W. M. (2012) Relative contributions of local cell and passing fiber activation and silencing to changes in thalamic fidelity during deep brain stimulation and lesioning: a computational modeling study. *Journal of Computational Neuroscience* **32**, 499-519.

Tass, P., Smirnov, D., Karavaev, A., Barnikol, U., Barnikol, T., Adamchic, I., Hauptmann, C., Pawelcyzk, N., Maarouf, M., Sturm, V., Freund, H. J. and Bezruchko, B. (2010) The causal relationship between subcortical local field potential oscillations and parkinsonian resting tremor. *Journal of Neural Engineering* **7**, 1-16.

Taghva, A. S., Malone, D. A. and Rezai, A. R. (2013) Deep brain stimulation for treatment-resistant depression. *World Neurosurgery* **80**, S17-S27.

Udupa, K. and Chen, R. (2015) The mechanisms of action of deep brain stimulation and ideas for the future development. *Progress in Neurobiology* **133**, 27-49.

Vargas-Irwin, C. and Donoghue, J. P. (2007) Automated spike sorting using density grid contour clustering and subtractive waveform decomposition. *Journal of Neuroscience Methods* **164**, 1-18.

Vonck, K., Sprengers, M., Carrette, E., Dauwe, I., Miatton, M., Meurs, A., Goossens, L., Herdt, V., Achten, R., Thiery, E., Raedt, R., Roost, D. and Boon, P. (2013) A decade of experience with deep brain stimulation for patients with refractory medial temporal lobe epilepsy. *International Journal of Neural Systems* **23**, 1-13.

Wang, Z., Feng, Z. and Wei, X. (2018) Axonal stimulations with a higher frequency generate more randomness in neuronal firing rather than increase firing rates in rat hippocampus. *Frontiers in Neuroscience* **24**, 1-11.

Yu, Y., Feng, Z., Cao, J., Guo, Z., Wang, Z., Hu, N. and Wei, X. (2016) Modulation of local field potentials by high-frequency stimulation of afferent axons in the hippocampal CA1 region. *Journal of Integrative Neuroscience* **15**, 1-17.